ELSEVIER
Journal of Power Sources 81–82 (1999) 867–871
JOURNAL OF POWER SOURCES
www.elsevier.com/locate/jpowsour

Testing of lithium-ion 18650 cells and characterizing/predicting cell performance

J.P. Fellner [a,*], G.J. Loeber [a], S.S. Sandhu [b]

[a] Air Force Research Laboratory, Propulsion Directorate, 1950 Fifth Street, Wright-Patterson AFB, OH 45433-7251, USA
[b] Department of Chemical and Materials Engineering, University of Dayton, Dayton, OH 45469-0246, USA

Abstract

The performance of lithium-ion cells, as determined from in-house testing, is primarily a function of cell design/materials, charge/discharge rate, ambient temperature, and the number of charge/discharge cycles. Testing of lithium-ion 18650 cells was performed in order to characterize their behavior and to eventually predict the performance of lithium-ion cells of various sizes. AC impedance spectroscopy was used to determine the interfacial resistance of the lithium-ion cells as a function of temperature, state-of-charge, and cycle number. From these results, a nonisothermal mathematical model was developed and preliminary results are presented.

Keywords: Lithium-ion; Batteries; AC impedance spectroscopy; Rechargeable; Mathematical model; Interfacial resistance

1. Introduction

Commercially available lithium-ion rechargeable batteries are suitable for use in consumer applications such as cellular phones, camcorders, and portable computers. However, in the more demanding aerospace environments, longer cycle life and high performance at extreme temperatures are required [1,2]. The purpose of this in-house effort was to first determine and then eventually predict the performance of existing lithium-ion cells from a given manufacturer.

2. Experimental

Several 18650 lithium-ion cells were purchased from a given manufacturer and are similar in construction with other commercially available lithium-ion batteries [3]. Notable differences are; the cathode is a mixture of $LiNiO_2$ and $LiCoO_2$, the electrolyte is a mixture of PC, EC, and DMC with $LiPF_6$, and the anode is a mixture of two different carbons.

Electrochemical AC impedance measurements using an EG&G PAR Model 273A potentiostat/galvanostat with a Model 5210 lock-in amplifier were performed on the 18650 cells as received and during various states of charge, temperature, and cycle number.

Electrochemical cycling was performed at temperatures from −20 to +40°C with a constant external cell environment temperature maintained by the use of a Tenney Environmental temperature chamber. Cell case temperature was monitored by the use of a thermocouple. Cell charging was performed using a constant current of 1.0 A (~2.2 mA cm^{-2} or 'C'-rate) to a cell voltage of 4.1 V and then constant voltage at 4.1 V until a total charge time of 3 h was reached. Discharging was performed at a constant current of 0.1–4.0 A (0.22–8.9 mA cm^{-2}) to a cell cut-off voltage of 2.5 V.

3. Results and discussion

3.1. Discharge behavior

The performance of a lithium-ion 18650 cell at room temperature with 100% depth-of-discharge (DOD) and 40% DOD are given in Figs. 1 and 2, respectively. At 100% DOD, the cell retains over 80% of its initial capacity for >500 cycles. At 40% DOD, the cell is still cycling after 3500 cycles.

* Corresponding author. Tel.: +1-937-255-7770; Fax: +1-937-656-7529; E-mail: fellnejp@possum.appl.wpafb.af.mil

0378-7753/99/$ - see front matter
PII: S0378-7753(98)00238-9

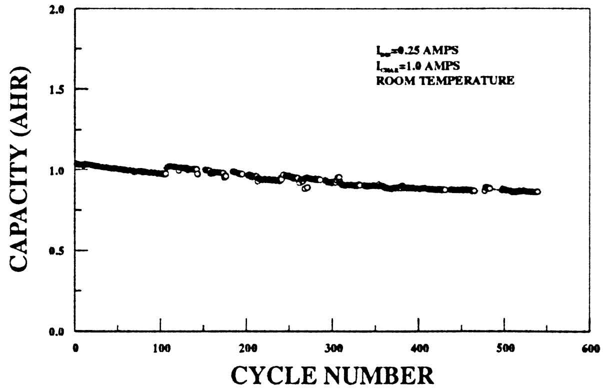

Fig. 1. Lithium-ion cell capacity vs. cycle number at room temperature.

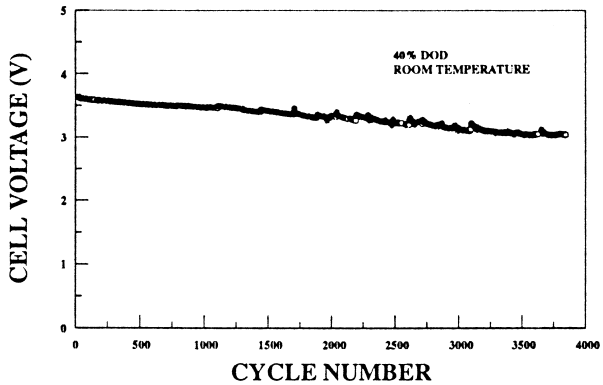

Fig. 2. Lithium-ion cell end-of-discharge cell voltage vs. cycle number at 40% depth-of-discharge and at room temperature.

The performance of a lithium-ion 18650 cell at room temperature early in its life (≤ 35 cycles), around cycle 150 at $T = 28.5$°C, and around cycle 450 at $T = -20$°C are given in Figs. 3–5, respectively. These data partially illustrate that the cell discharge performance behavior is complex and extremely sensitive to discharge rate, temperature, and cycle number.

The corresponding battery temperature for Figs. 4 and 5 as a function of discharge time and rate are given in Figs. 6 and 7, respectively. The battery is assumed to initially follow adiabatic heating. The solid straight lines in Figs. 6 and 7 then show the battery temperature under adiabatic heating conditions. Finite element calculations, shown later, indeed verify that this is a valid assumption.

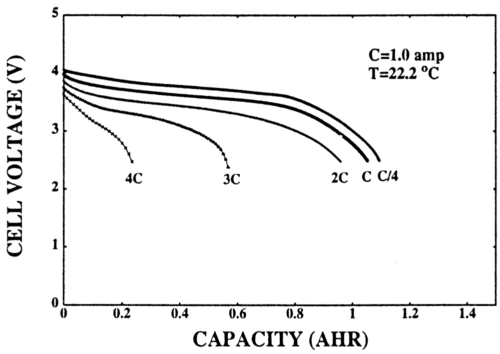

Fig. 3. Lithium-ion cell performance at room temperature at ≤ 35 cycles.

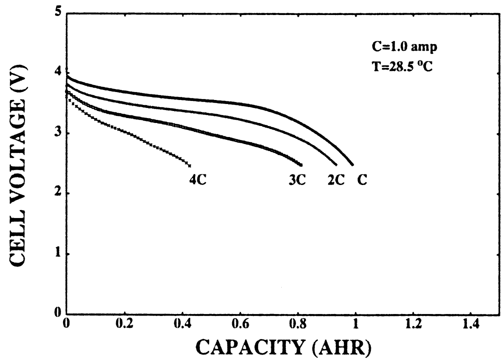

Fig. 4. Lithium-ion cell performance at $T = 28.5$°C around cycle number 150.

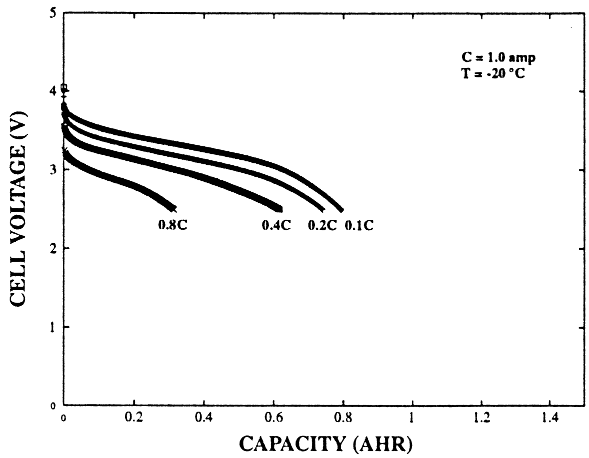

Fig. 5. Lithium-ion 18650 cell performance at $T = -20$°C around cycle number 450.

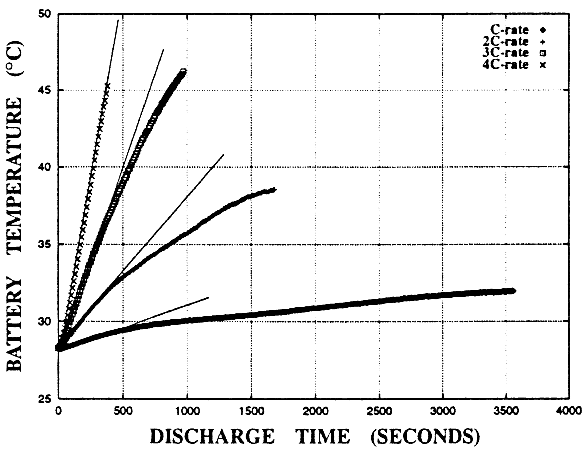

Fig. 6. Battery temperature vs. time at different discharge rates, initially at room temperature.

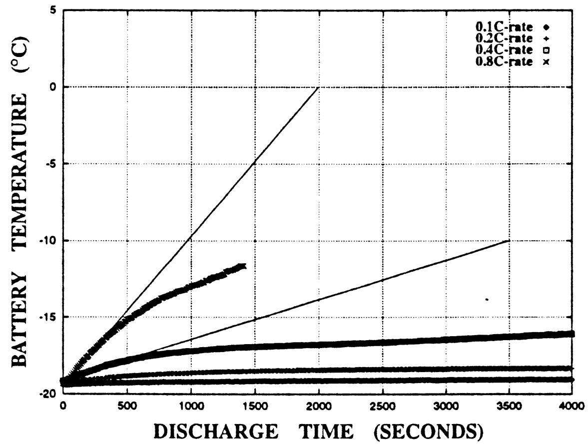

Fig. 7. Battery temperature vs. time at different discharge rates, initially $T = -20°C$.

3.2. Impedance behavior

In Fig. 8, the Nyquist plot for a discharged 18650 cell at a temperature of $T \simeq 10.0°C$ and at different cycle numbers are given. Note that the change in the high frequency intercept with the real axis is attributable to different AC impedance instrument leads/connectors as opposed to actual cell resistance changes.

The semi-circle portion of the Fig. 8 Nyquist plots (interfacial resistance) was plotted as a function of cycle number and temperature and are given in Fig. 9. Note that the data in Fig. 9 are from a single cell and that the two different straight lines illustrate that the interfacial resistance for a given cell is much higher at lower temperatures and the interfacial resistance appears to grow linearly with cycle number. Measuring a cell's impedance at different temperatures and cycle numbers can be used to diagnose the state-of-health of a given lithium-ion cell and as a tool for developing improved lithium-ion cells.

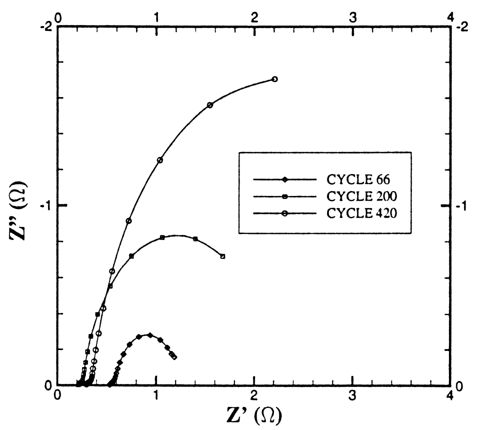

Fig. 8. Discharged Nyquist plot for a 18650 cell at $T \simeq 10.0°C$ and different cycle numbers.

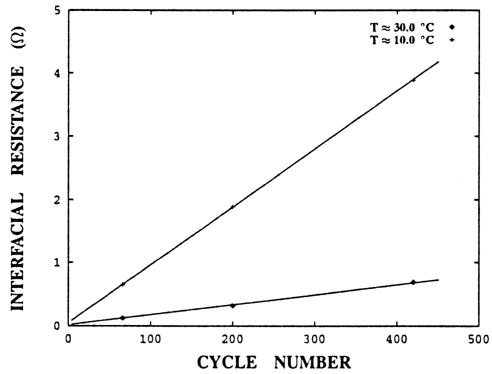

Fig. 9. Discharged interfacial resistance vs. cycle number and temperature.

The interfacial resistance at around cycle 60 as a function of state-of-charge and temperature is given in Fig. 10. Note that the logarithm of the interfacial resistance is linear with the inverse absolute cell temperature for a given state-of-charge, but Fig. 10 illustrates the tremendous changes in interfacial resistance with temperature more effectively. This interfacial resistance, represented by the depressed low frequency semi-circle, has been attributed to processes occurring at the anode electrode [4]. AC impedance on a lithium-ion cell with a reference electrode would be required to confirm this. Lithium-ion cells are a commercial success partly due to the very low interfacial resistance values at room temperature and above. Commercial lithium-ion cells also have a limited life partly due to the interfacial resistance increase with cycle number (shift of the Fig. 10 interfacial resistance curves to the upper right with cycle number).

Fig. 11 shows the Nyquist diagrams for the discharged 18650 cell at cycle 420 and various temperatures. The interfacial resistance from the Nyquist plots as a function of temperature is shown in Fig. 12. Note that the major change in impedance with temperature is attributable to the

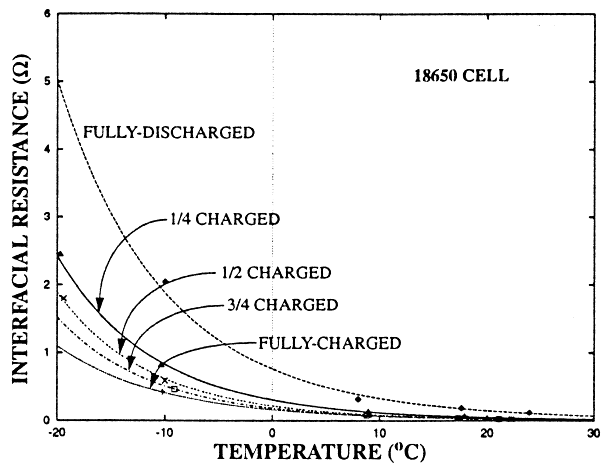

Fig. 10. Interfacial resistance as a function of temperature and state-of-charge at around cycle 60.

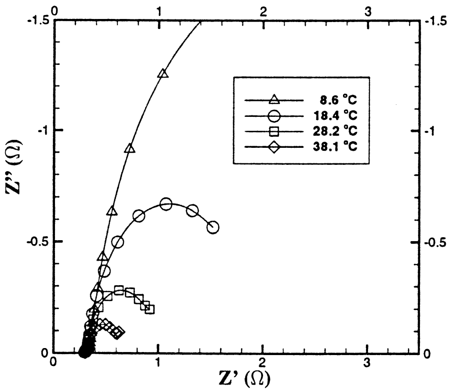

Fig. 11. Discharged Nyquist diagrams at various temperatures for cycle 420.

interfacial resistance. From the slope of Fig. 12, the activation energy for interfacial resistance is calculated to be 63.5 kJ mol^{-1}.

3.3. Thermal simulations

In Figs. 13–15, finite element simulations of the 18650 external cell temperature as function of discharge time, temperature, and free-convection heat transfer coefficient are given. Unlike the Sony-type cell [5], the entropic heating term for this lithium-ion cell, ΔS_{rev}, was found to be on the order of -3.8 J K^{-1} per g-mole of lithium as determined from open-circuit cell voltage measurements at different temperatures. The entropic heating is a minor amount at moderate to high discharge rates in relation to resistive heating and was subsequently neglected. The calculated heat capacity of the cell was on the order of 1.03 J g^{-1} K^{-1}. Estimated effective thermal conductivity values were calculated and utilized; however, temperature gradients within the cell were minimal. The internal heat generation values were based on the total discharge current and cell resistance values determined from AC impedance. At high temperatures and low cycle numbers, the interfacial resistance is small and the total cell resistance changes minimally with temperature. At low or high temperatures and high cycle numbers, however, the interfacial resistance is a substantial part of the total cell impedance and this

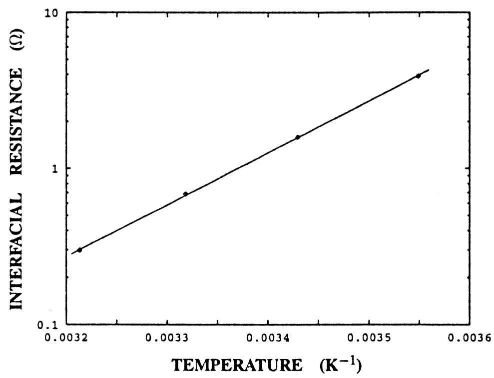

Fig. 12. Discharged interfacial resistance vs. temperature for cycle 420.

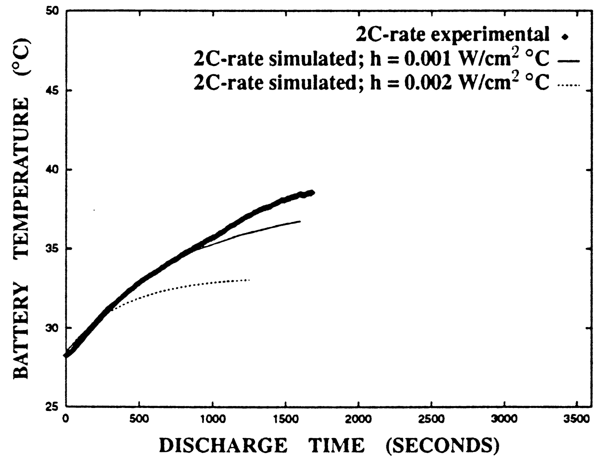

Fig. 13. Battery temperature, experimental and simulated, vs. discharge time at $T \simeq 28.5$°C and 2C.

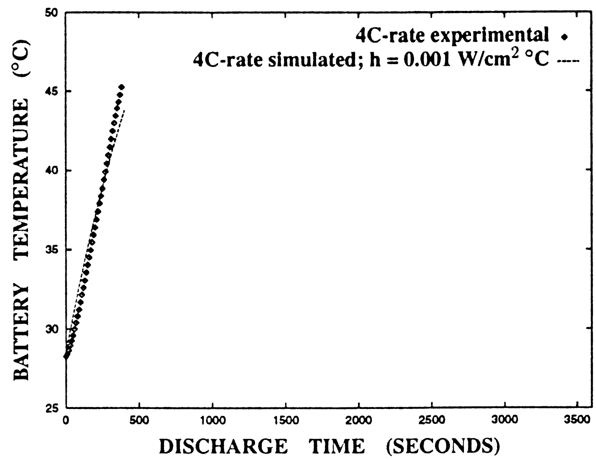

Fig. 14. Battery temperature, experimental and simulated, vs. discharge time at $T \simeq 28.5$°C and 4C.

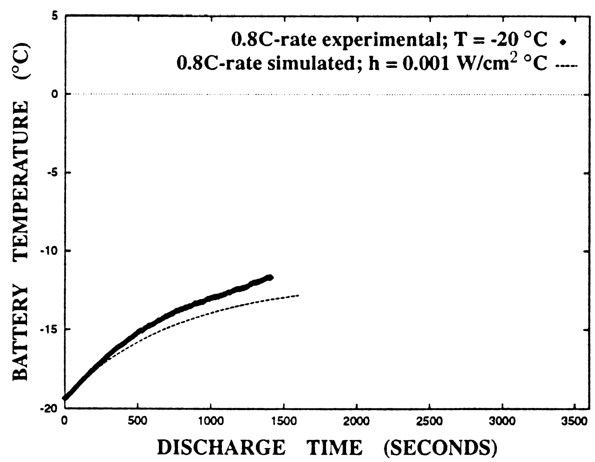

Fig. 15. Battery temperature, experimental and simulated, vs. discharge time at $T \simeq -19.8$°C and 0.8C.

resistance changes substantially as the cell discharges and the cell temperature increases. For Fig. 15, as a first approximation, an effective average resistance term based on the cell end temperatures was utilized.

These thermal simulations give a good engineering estimate of the cell temperature as a function of time at relatively high discharge rates. Further work needs to be performed in integrating the thermal simulations with transient mass transfer models and impedance modeling to predict the cell capacity as a function of temperature and discharge rate.

4. Conclusions

The capacity of a lithium-ion 18650 cell from a given manufacturer was found to be extremely sensitive to the charge/discharge rate, ambient cell temperature, and the number of charge/discharge cycles. Excellent cell performance is seen at room temperature and above; however, poor performance is seen at subambient temperatures such as $T = -20°C$. The cell temperature changes dramatically during discharge at high rates and the cell temperature can be approximated by assuming adiabatic heating.

The interfacial resistance increases linearly with cycle number. For a given cycle, the interfacial resistance increases with discharge and with decreasing temperature. For a given cycle and state-of-charge, the interfacial resistance increases exponentially with the inverse absolute cell temperature indicating an activated rate process such as solid-state diffusion and/or electrochemical kinetics.

For this type of lithium-ion cell, the contribution of the entropy term ΔS_{rev} may be neglected when performing thermal simulations for moderate to high discharge rates. At low or high temperatures and high cycle numbers, the interfacial resistance is a substantial part of the total cell impedance and this resistance needs to be accounted for in performing thermal and cell capacity mathematical modeling.

References

[1] D.A. Brewer, S. Surampudi, G. Halpert, 38th Power Sources Conference, Cherry Hill, NJ, 1998, pp. 97–100.

[2] R.A. Marsh, S.P. Vukson, Lithium-ion battery development program sol., PRDA No. 98-01-POK, Commerce Business Daily, PSA#1977, Nov. 21, 1997.

[3] B.A. Johnson, R.E. White, J. Power Sources 70 (1998) 48–54.

[4] M.J. Isaacson, M.E. Daman, R.P. Hollandsworth, Thirty-Second IECEC 1 (1997) 31–34.

[5] J. Hong, H. Maleki, S. Al Hallaj, L. Redey, J.R. Selman, J. Electrochem. Soc. 145 (1998) 1489–1501.